

Study of the structure of stellar atmospheres with VLT/AMBER

I. Martí-Vidal^{1,2} and J. M. Marcaide²

¹ Max-Planck-Institut für Radioastronomie, Bonn (Germany)

² Dpt. Astronomia i Astrofísica, Universitat de València (Spain)

Abstract

We report on *K*-band VLT/AMBER observations at medium spectral resolution (~ 1500) of RS Capricorni, an M6/M7III semi-regular AGB star. From the spectrally-dispersed visibilities, we measure the star diameter as a function of observing wavelength from 2.13 to 2.47 microns. We detect size variations of around 10% in the CO band heads, indicating strong opacity effects of CO in the stellar atmosphere. We also detect a linear increase of the size as a function of wavelength, beginning at 2.29 microns. Models of the stellar atmosphere, based on the mass of the star as estimated from stellar-evolution models, predict CO-size effects about half of those observed, and cannot reproduce the linear size increase with wavelength, for wavelengths longer than 2.29 microns. We are able to model this linear size increase with the addition of an extended water-vapor envelope around the star. We also find evidence of an additional extended CO envelope.

1 Introduction

The effective size of a star at a given wavelength depends on the opacity of the stellar atmosphere at that wavelength. Since we effectively measure the diameter of the $\tau = 1$ surface of the star, the size is related to the extension of the atmospheric region where the absorption is produced. The diameter of that surface varies with opacity and therefore with frequency. The atmospheres of cool giants are so extended that these size variations are observable with an interferometer. [10] and [11] studied the extended absorption regions of stellar atmospheres of cool giant stars in the TiO band at 712 nm with the MkIII interferometer. These authors measured the visibilities of a set of 47 stars using two filters, one centered in the TiO band, and the other in the continuum part of the spectrum close to the TiO band (754 nm). They found that the sizes in the TiO band are larger than those in the continuum, and that this effect is stronger for cooler stars. The sizes in the TiO absorption band are $\sim 10\%$ larger

than in the continuum for $R - I$ color indices of ~ 1.6 (spectral types M3–M4) and as much as 30% larger for $R - I$ color indices of ~ 2.2 (spectral types M6–M7).

Similar differences between the size observed in the continuum and the size observed in bands containing absorption band heads of other molecules (like H₂O or CO) have been reported for AGB stars. [6] and [7], for instance, reported very large size ratios (50% or more) for some stars.

[10] and [11] were successful in qualitatively reproducing their data with the latest set of cool giant models from the general-purpose stellar atmosphere code PHOENIX. Spherical, hydrostatic, massively line-blanketed atmosphere models were constructed and used to predict the uniform-disk diameters in the TiO band and in the continuum band as a function of model effective temperature, surface gravity, and mass (the stellar mass was used in the modelling, since it controls the deviation from plane-parallel atmospheres.) For most of the observed oxygen-rich giants, the diameter ratios between the TiO band and the continuum band agreed with the models computed for masses $\sim 0.5 M_{\odot}$. Hence, model atmospheres with very low stellar masses could fit the large diameter ratios observed in many stars, although evolutionary models predict masses as large as $5 M_{\odot}$.

A possible explanation of this inconsistency would be the existence of a transition zone at the base of the stellar wind (the *MOLsphere*; e.g. [14], and references therein), which could provide sufficient opacity in the TiO bands (and other molecular bands) to make AGB stars appear much larger than predicted by the hydrostatic model atmospheres like PHOENIX. According to this picture, one would expect similar size effects for the CO band heads. Therefore, we decided to use AMBER in the K band to measure the effective sizes of a set of four cool giant stars through the CO band heads at $2.3 \mu\text{m}$. The use of AMBER in medium-resolution mode ($\lambda/\Delta\lambda \sim 1500$) provides considerably more information than could be obtained with the MkIII interferometer [10] and the IOTA interferometer [6, 7], in which narrow-band filters were used. In this contribution, we report on the results obtained from the analysis of the observations of the first star of our sample: RS Cap.

RS Cap (HD 200994) has a K -band magnitude of -0.2 [1]. It is a semi-regular variable (SRb) of spectral type M6/M7III and is located at $\alpha = 21\text{h } 07\text{m } 15.4\text{s}$, $\delta = -16^{\circ} 25' 21.4''$ (J2000.0). A variability amplitude of $\Delta V \sim 0.5$ is seen in the Hipparcos data [8], although a larger variability amplitude (in photometric magnitude) of $\Delta B \sim 2$ was reported in [4], with a period of ~ 340 days.

2 AMBER observations of RS Cap

We observed star RS Cap with the ESO Very Large Telescope Interferometer (VLTI) using the Astronomical Multi-BEam combineR, AMBER (see [9] for details on this instrument), in medium-resolution mode ($\lambda/\Delta\lambda \sim 1500$). This instrument allows to perform simultaneous observations of the interferometric fringes generated by three telescopes. Therefore, it allows to measure *closure phases*, which are quantities independent of atmospheric or instrumental telescope-dependent contributions, e.g., [13]. The large spectral coverage of our observing mode contains the ¹²CO (2–0), (3–1), and (4–2), as well as the ¹³CO (2–0) band heads,

together with the continuum blueward of the ^{12}CO (2–0) band head at $2.29\ \mu\text{m}$. The details of the instrument configuration, observing schedule, and data calibration (both photometric and interferometric) is described in [5].

3 Results and discussion

3.1 Continuum angular diameter and effective temperature

In Fig. 1, we show (a) the normalized spectrum of RS Cap, (b) the amplitude visibilities for the three baselines (higher visibility corresponds to shorter baseline), and (c) the resulting diameter estimates obtained from the fit of a uniformly-bright disk to the visibilities at each spectral channel.

There are two clear aspects in the region of CO first overtone bands ($\lambda > 2.3\ \mu\text{m}$) which are worth noticing. On the one hand, we see an increase of $\sim 10\%$ of size in all the CO band heads, compared to the sizes in the continuum. On the other hand, there is a linear trend of increasing size with observing wavelength, beginning on $2.29\ \mu\text{m}$. Due to this latter effect, the size in the continuum at $2.45\ \mu\text{m}$ is $\sim 12\%$ larger than the size in the continuum for the wavelengths shorter than $2.29\ \mu\text{m}$.

The best-fit Rosseland diameter of RS Cap is $\theta_{\text{Ross}} = 7.95 \pm 0.07$. This diameter is compatible with that reported in [12] from lunar occultations and that reported in [2] from IOTA observations, although the precision in our estimate is a factor 10 higher. Our size estimate, together with the bolometric flux of $(2.1 \pm 0.2) \times 10^{-6}\ \text{erg cm}^{-2}\ \text{s}^{-1}$ reported in [12], translates into an effective temperature of $T_{\text{eff}} = 3160 \pm 160\ \text{K}$.

3.2 Atmosphere modeling

We compared the observed CO size effects in RS Cap with different model atmospheres computed with the MARCS code, e.g., [3]. The MARCS code computes the hydrostatic atmospheric structure in radiative and convective equilibrium for spherical atmosphere with molecular and atomic lines taken into account using the Opacity Sampling method. Each model in spherical geometry (suitable for AGB stars) is specified by several parameters. For the case of RS Cap, we have an effective temperature of $T_{\text{eff}} = 3200\ \text{K}$, a surface gravity of $\log g = 0.0$, a stellar mass of $M = 2 M_{\odot}$, and a moderately CN-cycled chemical composition. See [5] for a discussion on the different parameters used to model our observations of RS Cap.

We show in Fig. 2 a comparison between observed visibilities (black lines) and those computed from the MARCS model. The relatively large depth of the features of the CO band heads cannot be reproduced by the model. Additionally, the observed visibility amplitudes at wavelengths longer than $\sim 2.29\ \mu\text{m}$ are systematically lower than the model predictions; this difference between model and observations is larger for longer wavelengths. In other words, the effective size of the star at wavelengths longer than $\sim 2.29\ \mu\text{m}$ is systematically larger than the effective size derived from the MARCS model.

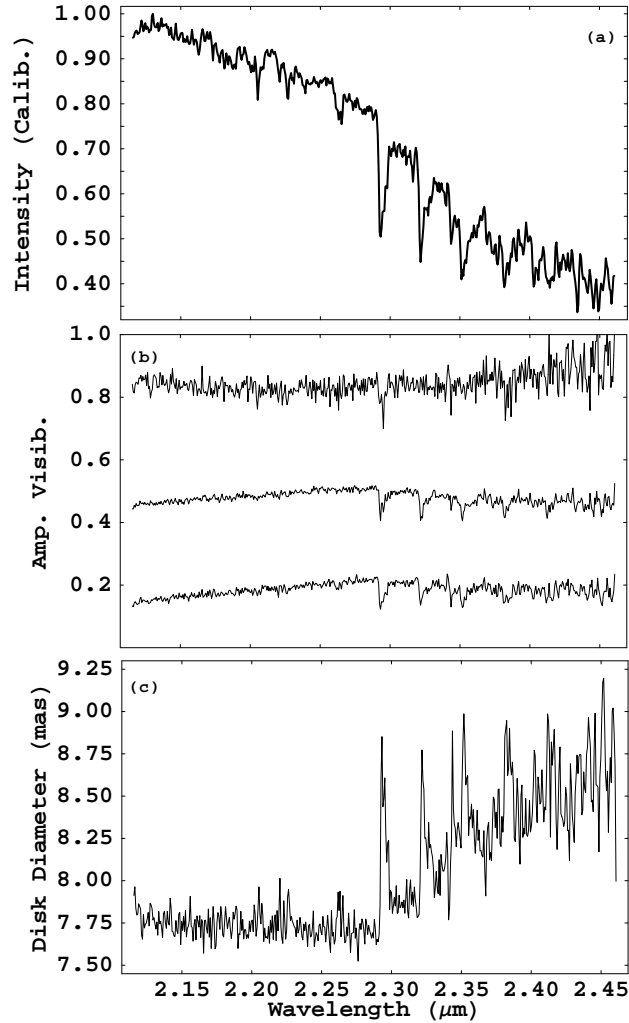


Figure 1: (a) Spectrum of RS Cap (normalized); (b) calibrated visibility amplitudes; (c) uniform-disc angular diameter at each AMBER spectral channel.

3.2.1 Additional water-vapor envelope

An extra contribution must be added to the MARCS models to fit the visibilities in the observed spectral range. We can reproduce the lower visibility amplitudes (i.e., the larger effective sizes) beyond $2.29 \mu\text{m}$ by adding a contribution to the stellar opacity due to water vapor around the star. The opacity corresponding to the wide absorption of water vapor centered at $\sim 2.7 \mu\text{m}$ may account for the larger angular sizes observed at the longer wavelengths. We added a simple water-vapor model envelope to the MARCS pressure/density profiles, consisting of a fitted narrow spherical shell with a radius of 2 and a width of 0.1 (both in units of the stellar radius), a column density of 10^{21} cm^{-2} , and a temperature of 1500 K. Using these parameters, we are able to fit the amplitude visibilities at $\lambda > 2.29 \mu\text{m}$, as we show in Fig. 2

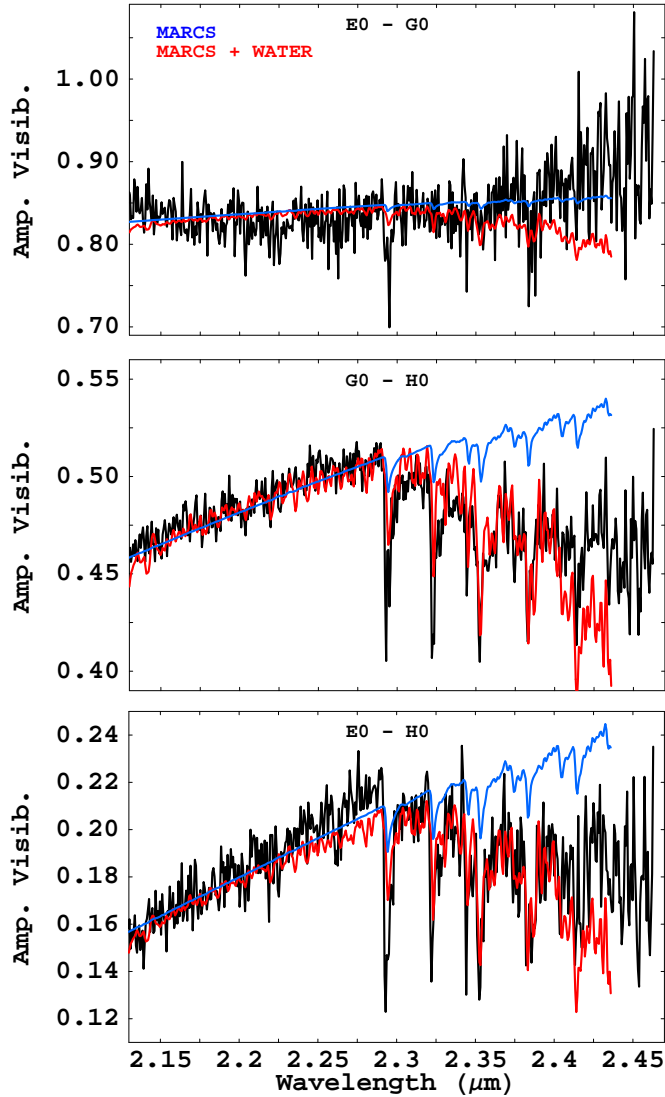


Figure 2: *Black*: AMBER visibilities of RS Cap for our three baselines (from short to long: E0-G0, G0-H0, and E0-H0). *Blue*: model visibilities, computed using a MARCS model (see text). *Red*: model visibilities, computed from the MARCS model and a water-vapor envelope (see text).

(red lines). With this model, we obtain $\chi_{\text{red}}^2 = 8.1$. This large reduced χ^2 is partially due to the discrepancy in the CO bands, which is discussed in the next subsection. Our model follows the general trend of decreasing visibility amplitudes for wavelengths longer than $2.3 \mu\text{m}$, although underestimates the visibility amplitudes at wavelengths longer than $2.4 \mu\text{m}$.

The presence of dense water vapor envelopes in semi-regular or irregular (i.e., non-

Mira-type) AGB stars was first revealed by [15], who unmasked the $2.7 \mu\text{m}$ water vapor band originating in the dense molecular layers extending to ~ 2 stellar radii. Based on infrared interferometric observations, [6] found an increase in the angular size by 30–60% between the K and L' band in five semi-regular AGB stars, which the authors interpreted as due to the emission from the extended molecular layers. But they used the broadband filters which are not capable of spectrally resolving the water vapor bands. Our AMBER measurements are the first study to *spatially and spectrally* resolve the water vapor emission from the dense molecular layers for a semi-regular AGB star.

It is worth noting that a similar increase of the angular diameter longward of $2.3 \mu\text{m}$ is found in Mira stars as well [7, 16]). The shock wave in Miras is generated by the periodic, large-amplitude pulsation. Therefore, the shock in non-Mira stars with much smaller variability amplitude is expected to be much weaker. However, despite the striking difference in the variability amplitude ($\Delta V = 6\text{--}9$ and $0.5\text{--}2$ for Miras and RS Cap, respectively), the semi-regular AGB star RS Cap produces a warm water vapor envelope similar to that of Miras. At the moment, there is no straightforward explanation for the origin of this warm water envelope in RS Cap.

3.2.2 Additional CO envelope

The low visibility amplitudes at the CO band heads hint to an extended envelope of CO around the star. For instance, if $\sim 20\%$ of the emission in the CO band head at $2.29 \mu\text{m}$ would come from a very extended envelope of, say, ~ 20 mas radius or larger, it would map into a decrease in the visibility amplitude that would roughly match the observations in that part of the spectrum. Unfortunately, we do not have enough data to be able to characterize well this possible extra component of CO absorption.

4 Conclusions

We have observed the AGB star RS Cap with VLTI/AMBER in the K band with medium-resolution mode (506 channels between 2.13 and $2.47 \mu\text{m}$). We estimate a Rosseland diameter of 7.95 ± 0.07 mas in the continuum, which translates into an effective temperature of 3200 ± 160 K. The apparent size of the star increases monotonically by $\sim 12\%$ between 2.29 and $2.47 \mu\text{m}$. We have detected lower than expected visibility amplitudes in all the CO band heads observed. These lower amplitudes translate into larger apparent sizes of the star in the CO band heads.

We have used MARCS atmospheric models to generate synthetic visibilities and compare them directly to our AMBER observations. We are not able to reproduce the low visibility amplitudes in the CO band heads. The discrepancy between models and observations in the CO band heads might be resolved either by using a much lower mass for RS Cap (below $1 M_{\odot}$, thus in contradiction with the stellar-evolution models) or by an envelope of CO around the star. Additionally, to fit the observations at wavelengths longer than $2.29 \mu\text{m}$, we must add an *ad hoc* narrow spherical water-vapor envelope, similar to the models used in [7]. We model

this envelope with a temperature of 1500 K, a size of twice that of the star, a width of 0.1 times the stellar radius, and a column density of 10^{21} cm⁻².

Acknowledgments

I. Martí-Vidal is a fellow of the Alexander von Humboldt Foundation in Germany. Partial support from Spanish grants AYA-2006-14986-C02 and Prometeo 2009/104 is acknowledged. This work is based on observations made with ESO Telescopes at the Paranal Observatory under programme ID 383.D-0619.

References

- [1] Cutri, R.M., Skrutskie, M.F., van Dyk, S., et al. 2003, The IRSA 2MASS All-Sky Point Source Catalog, NASA/IPAC Infrared Science Archive
- [2] Dyck, H.M., van Belle, G.T., & Thompson, R.R. 1998, *AJ*, 116, 981
- [3] Gustafsson B., Edvardsson B., Eriksson K., et al. 2008, *A&A* 486, 951
- [4] Kukarkin, B.V., Kholopov, P.N., Efremov, Yu.N., et al. 1969, General Catalog of Variable Stars, Academy of Sciences of the USSR, Moscow
- [5] Martí-Vidal, I., Marcaide, J.M., Quirrenbach, A. et al. 2011, *A&A*, 529, 115
- [6] Mennesson, B., Perrin, G., Chagnon, G., et al. 2002, *ApJ*, 579, 446
- [7] Perrin, G., Ridgway, S. T., Mennesson, B., et al. 2004, *A&A*, 426, 279
- [8] Perryman, M.A.C., & ESA 1997, The Hipparcos and Tycho catalogues, Noordwijk (Netherlands, ESA Publications Division), ESA SP Ser. Vol 1200
- [9] Petrov, R.G., Malbet, F., Weigelt, G., et al., *A&A*, 464, 1
- [10] Quirrenbach, A., Mozurkewich, D., Armstrong, J.T., et al. 1993, *ApJ*, 406, 215
- [11] Quirrenbach, A., Mozurkewich, D., Armstrong, J.T., et al. 2001, *BAAS*, 33, 882
- [12] Richichi, A., Di Giacomo, A., Lisi, F., & Calamai, G. 1992, *A&A*, 265, 535
- [13] Rogers A.E.E., Hinteregger H.F., Whitney A.R., et al. 1974, *ApJ*, 193, 293
- [14] Tsuji, T. 2008, *A&A*, 489, 1271
- [15] Tsuji, T., Ohnaka, K., Aoki, W., & Yamamura, I. 1997, *A&A*, 320, L1
- [16] Wittkowski, M., Boboltz, D. A., Driebe, T., Le Bouquin, J.-B., Millour, F., Ohnaka, K., & Scholz, M. 2008, *A&A*, 479, L21